International Journal of Fracture **77**: 77–93, 1996.

Asymptotic solution for mode III crack growth in J_2-elastoplasticity with mixed isotropic-kinematic strain hardening

D. BIGONI[1] and E. RADI[2]
[1] *Istituto di Scienza delle Costruzioni, University of Bologna, V. le Risorgimento 2, 40136 Bologna, Italy*
[2] *Istituto di Ingegneria, University of Ferrara, Via Saragat 1, 44100 Ferrara, Italy*

Received 22 May 1995; accepted 9 January 1996

Abstract. Mode III fracture propagation is analyzed in a J_2-flow theory elastoplastic material characterized by a mixed isotropic/kinematic law of hardening. The asymptotic stress, back stress and velocity fields are determined under small-strain, steady-state, fracture propagation conditions. The increase in the hardening anisotropy is shown to be connected with a decrease in the thickness of the elastic sector in the crack wake and with an increase of the strength of the singularity. A second order analytical solution for the crack fields is finally proposed for the limiting case of pure kinematic hardening. It is shown that the singular terms of this solution correspond to fully plastic fields (without any elastic unloading sector), which formally are identical to the leading order terms of a crack steadily propagating in an elastic medium with shear modulus equal to the plastic tangent modulus in shear.

1. Introduction

There is no need to emphasize the conceptual and practical importance of the J_2-flow theory of plasticity. In the context of fracture mechanics, it may be noted that, since the appearance of the fundamental works by Hutchinson [1, 2] and Rice and Rosengren [3], where a stationary crack was analyzed adopting the J_2-deformation theory of plasticity, a number of solutions of fracture problems have been obtained for J_2-type elastoplastic materials. As a matter of fact, even if the discussion is confined to asymptotic solution of steady-state, rectilinear fracture propagation problems, many contributions should be mentioned. In particular, fracture growth in perfectly plastic material was analyzed under mode III [4] and mode I, II [5, 6] (see the discussion by Rice [7]). In the case of linear isotropic hardening, Ponte Castañeda [8] was successful in generalizing the asymptotic analysis of Amazigo and Hutchinson [9] by including plastic reloading on crack flanks. Inspired by his solving technique, the authors have obtained solutions for fracture propagation in materials characterized by pressure-sensitive yielding with isotropic hardening [10–12] and, quite recently, with anisotropic hardening [13]. Despite the importance of employing an anisotropic hardening law to model the Bauschinger effect, which is commonly exhibited by ductile metals and alloys, the only available asymptotic solution for crack propagation in a material characterized by the J_2-flow theory with mixed isotropic/kinematic hardening is due to Zhang et al. [14], who analyzed mode I propagation. These results can be obtained as a particular case of a porous elastoplastic solid analyzed by the authors in [13], to which the interested reader is referred. However, an asymptotic solution for mode III is still lacking; this is obtained in the present paper.

We give the asymptotic solution for a crack propagating steadily under antiplane shearing conditions in a material obeying the J_2-flow theory of plasticity with a linear combination of isotropic and kinematic hardening. We seek the first order solution in the separable-variable

form proposed in [9], which, in addition to stress and velocity fields, is extended to represent the internal variables governing the hardening behaviour.

We take into account elastic unloading and subsequent plastic reloading in the crack wake by using the technique proposed in [8]. This can be considered appropriate under the hypothesis of the infinitesimal theory, where the trajectories of the material points, with respect to the crack tip, can be approximated as rectilinear.

The results obtained are consistent with the finite element simulation of mode III crack growth of Narasimhan et al. [15] and show that the kinematical component of hardening plays an important role on the crack-tip field. Among other effects of the hardening anisotropy, we note that the solution tends to a solution corresponding to a crack steadily propagating in an elastic medium in the limiting case of pure kinematic hardening. Aiming to clarify this issue, we solve analytically the case of pure kinematic hardening, employing a higher order representation of crack-tip fields. In this limiting case, it is shown that no elastic unloading occurs in the crack wake. Moreover, the most singular crack-tip fields are identical to the corresponding fields of a crack propagating in an isotropic elastic medium having shear modulus equal to the plastic tangent modulus in shear. The solution represents the first effort to obtain a second order solution for crack-propagation in elastoplasticity.

2. Constitutive model

The J_2-flow theory of plasticity is based on the constitutive assumptions which are summarized in this section. Yielding can occur for stress states lying on the von Mises yield surface

$$f(\tilde{\boldsymbol{\sigma}}, k) = \tfrac{3}{2}|\mathrm{dev}\,\tilde{\boldsymbol{\sigma}}|^2 - \sigma_e^2 = 0, \tag{1}$$

where dev is the linear operator which associates to any second order tensor its deviatoric component ($\forall \mathbf{X} \in$ Lin, $\mathrm{dev}\,\mathbf{X} = \mathbf{X} - (\mathrm{tr}\,\mathbf{X})\mathbf{I}/3$, Lin being the set of second order tensors and tr denoting the trace), σ_e is the yield stress under unixial tension proportional to the radius of the current yield surface by a factor $\sqrt{\frac{3}{2}}$, and $\tilde{\boldsymbol{\sigma}}$ is the *reduced stress* tensor

$$\tilde{\boldsymbol{\sigma}} = \boldsymbol{\sigma} - \boldsymbol{\alpha}, \tag{2}$$

namely, the difference between the *stress* $\boldsymbol{\sigma}$ and the *back stress* $\boldsymbol{\alpha}$.

When the stress state satisfies the yield condition (1), the hardening variables σ_e and $\boldsymbol{\alpha}$ have the following evolution laws

$$\dot{\boldsymbol{\alpha}} = (1-b)\frac{\langle \mathrm{dev}\,\tilde{\boldsymbol{\sigma}}\cdot\dot{\boldsymbol{\sigma}}\rangle}{|\mathrm{dev}\,\tilde{\boldsymbol{\sigma}}|^2}\tilde{\boldsymbol{\sigma}}, \tag{3}$$

$$\dot{\sigma}_e = b\frac{\langle \mathrm{dev}\,\tilde{\boldsymbol{\sigma}}\cdot\dot{\boldsymbol{\sigma}}\rangle}{|\mathrm{dev}\,\tilde{\boldsymbol{\sigma}}|^2}\sigma_e, \tag{4}$$

where $\dot{\boldsymbol{\sigma}}$ is the stress rate, and $b \in [0,1]$ is the parameter governing the *mixity* of hardening, i.e. $b = 0$ and $b = 1$ correspond to the extreme cases of pure kinematic and pure isotropic hardening. The Macaulay brackets $\langle\ \rangle$ denotes the operator $\mathbb{R} \to \mathbb{R}^+ \cup \{0\}, \forall x \in \mathbb{R}, \langle x\rangle = (x + |x|)/2$.

It should be noted that the Prager [16] and Ziegler [17] hardening rules coincide in the present context, where the von Mises yield function and the associative flow rule have been

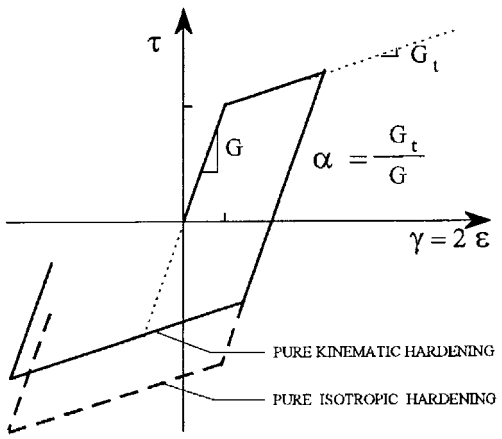

Figure 1. Isotropic and kinematic hardening models: uniaxial stress-strain response in shear.

adopted. Moreover, Prager consistency [18] is automatically satisfied by (3) and (4), which represent a *linear combination* of isotropic and kinematic hardening.

The total deformation rate is the sum of the elastic and plastic parts

$$\dot{\varepsilon} = \dot{\varepsilon}^e + \dot{\varepsilon}^p, \tag{5}$$

and the incremental elastic and plastic constitutive laws are

$$2G\dot{\varepsilon}^e = \dot{\boldsymbol{\sigma}} - \frac{\nu}{1+\nu}(\mathrm{tr}\,\dot{\boldsymbol{\sigma}})\mathbf{I}, \tag{6}$$

$$2G\dot{\varepsilon}^p = \frac{1-\alpha}{\alpha}\frac{\langle \mathrm{dev}\,\tilde{\boldsymbol{\sigma}}\cdot\dot{\boldsymbol{\sigma}}\rangle}{|\mathrm{dev}\,\tilde{\boldsymbol{\sigma}}|^2}\,\mathrm{dev}\,\tilde{\boldsymbol{\sigma}}, \tag{7}$$

where ν is the Poisson ratio and α is the ratio of the tangent modulus in shear G_t to the elastic shear modulus G. The coefficient α is assumed *constant* and *strictly positive* (strain softening and perfectly plastic behaviors are excluded) and can be directly related to the response of material in pure shear (Figure 1).

Equations (1), (3–8), completely specify the elastoplastic material behavior.

3. Mode III propagation

We consider a mode III rectilinear fracture growth problem, in which a crack propagates at constant velocity in an infinite medium. The medium is characterized by the J_2-flow theory of plasticity with linear mixed isotropic/kinematic hardening. In a cylindrical coordinate system r, ϑ, x_3, moving with the crack tip towards $\vartheta = 0$ and having the x_3-axis directed along the straight crack front, the only non zero stress, back stress and velocity components are, in antiplane shearing, $\sigma_{3r}, \sigma_{3\vartheta}, \alpha_{3r}, \alpha_{3\vartheta}$ and v_3. Therefore, the stress and back stress tensors are deviatoric, i.e.: $\mathrm{dev}\,\boldsymbol{\sigma} = \boldsymbol{\sigma}$, $\mathrm{dev}\,\tilde{\boldsymbol{\sigma}} = \tilde{\boldsymbol{\sigma}}$.

3.1. Field equations

Under mode III loading conditions, the quasistatic *equilibrium equations* reduce to

$$r\sigma_{3r,r} + \sigma_{3\vartheta,\vartheta} + \sigma_{3r} = 0, \tag{8}$$

and the *constitutive equations* (3–7) to

$$2G\dot{\varepsilon}_{3r} = \dot{\sigma}_{3r} + \gamma(\alpha^{-1} - 1)\tilde{\sigma}_{3r}, \qquad 2G\dot{\varepsilon}_{3\vartheta} = \dot{\sigma}_{3\vartheta} + \gamma(\alpha^{-1} - 1)\tilde{\sigma}_{3\vartheta}, \tag{9}$$

$$\dot{\alpha}_{3r} = \gamma(1 - b)\tilde{\sigma}_{3r}, \qquad \dot{\alpha}_{3\vartheta} = \gamma(1 - b)\tilde{\sigma}_{3\vartheta}, \qquad \dot{\sigma}_e = b\gamma\sigma_e, \tag{10}$$

where

$$\gamma = \frac{\langle \tilde{\sigma}_{3r}\dot{\sigma}_{3r} + \tilde{\sigma}_{3\vartheta}\dot{\sigma}_{3\vartheta} \rangle}{\tilde{\sigma}_{3\vartheta}^2 + \tilde{\sigma}_{3r}^2}. \tag{11}$$

The strain rate components are related to the out-of-plane velocity through the *kinematic compatibility conditions*

$$\dot{\varepsilon}_{3r} = \tfrac{1}{2}v_{3,r}, \qquad \dot{\varepsilon}_{3\vartheta} = \frac{1}{2r}v_{3,\vartheta}. \tag{12}$$

The steady-state condition yields the following *time derivative rule*, for stress rates

$$\begin{aligned} \dot{\sigma}_{3r} &= \frac{c}{r}\left[(\sigma_{3r,\vartheta} - \sigma_{3\vartheta})\sin\vartheta - r\sigma_{3r,r}\cos\vartheta\right], \\ \dot{\sigma}_{3\vartheta} &= \frac{c}{r}\left[(\sigma_{3\vartheta,\vartheta} + \sigma_{3r})\sin\vartheta - r\sigma_{3\vartheta,r}\cos\vartheta\right], \end{aligned} \tag{13}$$

and for the rates of hardening variables

$$\begin{aligned} \dot{\alpha}_{3r} &= \frac{c}{r}\left[(\alpha_{3r,\vartheta} - \alpha_{3\vartheta})\sin\vartheta - r\alpha_{3r,r}\cos\vartheta\right], \\ \dot{\alpha}_{3\vartheta} &= \frac{c}{r}\left[(\alpha_{3\vartheta,\vartheta} + \alpha_{3r})\sin\vartheta - r\alpha_{3\vartheta,r}\cos\vartheta\right], \\ \dot{\sigma}_e &= \frac{c}{r}\left(\sigma_{e,\vartheta}\sin\vartheta - r\sigma_{e,r}\cos\vartheta\right), \end{aligned} \tag{14}$$

where c is the (constant) crack-tip speed.

Equations (12–14) can be substituted into (9) and (10) to obtain, together with (8), a system of six PDEs for the six unknowns functions $\sigma_{3r}, \sigma_{3\vartheta}, v_3, \alpha_{3r}, \alpha_{3\vartheta}$, and σ_e. The PDEs system can be reduced to a system of ODEs when a solution is sought of the separable variable form proposed in [9]

$$\begin{aligned} \sigma_{3r}(r,\vartheta) &= G\left(\frac{r}{B}\right)^s T_r(\vartheta), \qquad \sigma_{3\vartheta}(r,\vartheta) = G\left(\frac{r}{B}\right)^s T_\vartheta(\vartheta), \\ \alpha_{3r}(r,\vartheta) &= G\left(\frac{r}{B}\right)^s A_r(\vartheta), \qquad \alpha_{3\vartheta}(r,\vartheta) = G\left(\frac{r}{B}\right)^s A_\vartheta(\vartheta), \\ v_3(r,\vartheta) &= \frac{c}{s}\left(\frac{r}{B}\right)^s w(\vartheta), \qquad \sigma_e(r,\vartheta) = \frac{c}{s}\left(\frac{r}{B}\right)^s T_e(\vartheta), \end{aligned} \tag{15}$$

where s is the exponent of the fields singularity and B denotes any characteristic dimension of the plastic zone. Having assumed the representations (15), the angular functions

$T_r, T_\vartheta, w, A_r, A_\vartheta, T_e$ and the field singularity s become the unknowns of the problem (the present asymptotic problem is homogeneous and thus the amplitude factor B remains undetermined). The representations (15) may be considered the most singular term in an asymptotic expansion of the near crack-tip fields.

By substituting (12–14) into (8–10) and employing the representation (15), we obtain the final system of ODEs

$$T_{\vartheta,\vartheta} = -(1+s)T_r, \tag{16.1}$$

$$T_{r,\vartheta} \sin\vartheta = T_\vartheta \sin\vartheta + sT_r \cos\vartheta + \Sigma_r, \tag{16.2}$$

$$w_{,\vartheta} = s\left(\Sigma_\vartheta + \frac{\lambda}{h}\tilde{T}_\vartheta\right), \tag{16.3}$$

$$A_{r,\vartheta} \sin\vartheta = A_\vartheta \sin\vartheta + sA_r \cos\vartheta + \lambda(1-b)\tilde{T}_r, \tag{16.4}$$

$$A_{\vartheta,\vartheta} \sin\vartheta = -A_r \sin\vartheta + sA_\vartheta \cos\vartheta + \lambda(1-b)\tilde{T}_\vartheta, \tag{16.5}$$

$$T_{e,\vartheta} \sin\vartheta = (s\cos\vartheta + \lambda b)T_e, \tag{16.6}$$

where

$$\tilde{T}_\vartheta = T_\vartheta - A_\vartheta, \qquad \tilde{T}_r = T_r - A_r, \tag{17}$$

$$\Sigma_\vartheta = -s(T_r \sin\vartheta + T_\vartheta \cos\vartheta), \qquad \Sigma_r = \left(w - \frac{\lambda}{h}\frac{\tilde{T}_r\tilde{T}_\vartheta}{T_e^2}\Sigma_\vartheta\right)\left(1 + \frac{\lambda}{h}\frac{\tilde{T}_r^2}{T_e^2}\right)^{-1}, \tag{18}$$

$$h = \frac{\alpha}{1-\alpha}, \tag{19}$$

and parameter λ is defined in such a way that the plastic loading and elastic unloading conditions are automatically accounted for, i.e.

$$\lambda = 3\frac{\langle \tilde{T}_\vartheta\Sigma_\vartheta + \tilde{T}_r\Sigma_r\rangle}{T_e^2}, \quad \text{if} \quad 3(\tilde{T}_r^2 + \tilde{T}_\vartheta^2) - T_e^2 = 0, \tag{20.1}$$

whereas

$$\lambda = 0, \quad \text{if} \quad 3(\tilde{T}_r^2 + \tilde{T}_\vartheta^2) - T_e^2 < 0. \tag{20.2}$$

With definition (20), Eqns. (16) become valid for plastic loading, neutral loading and elastic unloading. In (16), the singularity coefficient s is unknown and is to be determined as an eigenvalue of the nonlinear problem.

3.2. Boundary conditions

In order to solve system (16) for the unknown angular functions $T_r, T_\vartheta, w, A_r, A_\vartheta$, and T_e, the mode III boundary conditions are necessary. These are

$$\sigma_{3r}(r,0) = v_3(r,0) = 0, \qquad \sigma_{3\vartheta}(r,\pi) = 0, \tag{21}$$

or, in terms of angular functions

$$T_r(0) = w(0) = 0, \qquad T_\vartheta(\pi) = 0. \tag{22}$$

The initial boundary conditions on A_r, A_ϑ and T_e can be obtained by evaluating (16.4–16.6) at $\vartheta = 0$. In fact, since plastic loading occurs ahead of the crack tip, $T_e(0)$ does not vanish at $\vartheta = 0$, so (16.6) yields

$$\lambda(0) = -\frac{s}{b}. \tag{23}$$

Hence a substitution of (23) into (16.4) and (16.5), both evaluated at $\vartheta = 0$, yields

$$\begin{aligned} A_r(0) &= (1-b)T_r(0) = 0, \\ A_\vartheta(0) &= (1-b)T_\vartheta(0), \end{aligned} \tag{24}$$

which define the boundary conditions on A_r and A_ϑ as functions of the values assumed by the stress at $\vartheta = 0$. Finally, $T_e(0)$ can be obtained by (1), using representation (15)

$$T_e(0) = \sqrt{3}[T_\vartheta(0) - A_\vartheta(0)] = b\sqrt{3}T_\vartheta(0). \tag{25}$$

In order to avoid the trivial solution (the differential problem (16), with boundary conditions (22), is homogeneous), we assume $T_\vartheta(0) = 1$. Therefore, $A_\vartheta(0)$ is known from (24). A numerical integration of (16) can be preformed with a tentative value of s, which can be made precise by iterating on the basis of a check on (22.2).

3.3. Values of angular functions for small ϑ

Due to the term $\sin\vartheta$ multiplying the highest derivative term in (16.2) and (16.4–16.6), system (16) is singular at $\vartheta = 0$ and at $\vartheta = \pi$. The problem caused by the singularity at π can be easily overcome, noting that T_ϑ is well-behaved near π, and observing that the system of PDEs can be integrated to $\pi - \varepsilon$, where ε can be made as small as needed to obtain accurate results. In order to avoid the difficulty at $\vartheta = 0$, the integration has to be started at $\vartheta + \varepsilon$, with ε sufficiently small. This is possible if all angular functions are known at $\vartheta = \varepsilon$. These values of angular functions can be obtained through a Taylor series expansion at the origin. For this purpose, we need the values of the derivatives of angular functions evaluated at $\vartheta = 0$. From (16.1) and (16.3) the following two derivatives can be readily obtained

$$T_{\vartheta,\vartheta}(0) = 0, \qquad w_{,\vartheta}(0) = -\frac{s^2}{\alpha}. \tag{26}$$

If we differentiate with respect to ϑ both members of (16.2), (16.4), (16.5), and of (1), transformed with (15), and evaluate the resulting functions at $\vartheta = 0$, we obtain

$$\begin{aligned} T_{r,\vartheta}(0) &= 1 + s\tfrac{s-b}{s-\alpha b}, \\ A_{r,\vartheta}(0) &= (1-b)\left(1 + \tfrac{s^2}{s-\alpha b}\right), \\ A_{\vartheta,\vartheta}(0) &= 0, \\ T_{e,\vartheta}(0) &= 0. \end{aligned} \tag{27}$$

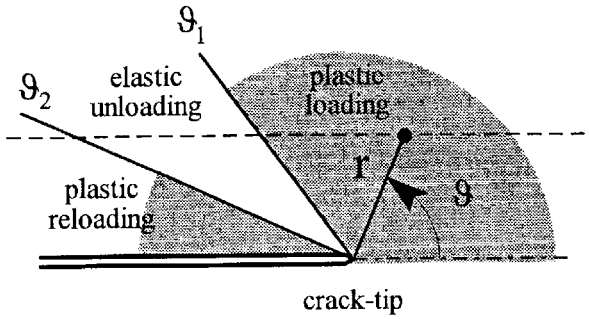

Figure 2. Plastic and elastic unloading sectors near a growing crack tip and loading history of a generic material point.

A Taylor series expansion of angular functions ahead of the crack tip yields the following values of functions at $\vartheta = \varepsilon$

$$\begin{aligned} T_\vartheta(\varepsilon) &= 1 + o(\varepsilon), \\ T_r(\varepsilon) &= \varepsilon T_{r,\vartheta}(0) + o(\varepsilon), \\ w(\varepsilon) &= \varepsilon w_{,\vartheta}(0) + o(\varepsilon). \\ A_\vartheta(\varepsilon) &= 1 - b + o(\varepsilon), \\ A_r(\varepsilon) &= \varepsilon A_{r,\vartheta}(0) + o(\varepsilon), \\ T_e(\varepsilon) &= \sqrt{3}b + o(\varepsilon), \end{aligned} \tag{28}$$

where the values of the derivatives at $\vartheta = 0$ are known from (26) and (27). It may be important to remark that (26–28) have been obtained under the hypothesis of non-singular behavior of angular functions at $\vartheta = 0$. This regularity condition may be justified by using physical arguments, as discussed in Appendix B of [19], for a similar crack propagation problem.

The numerical integration can, at this point, be performed by using the Runge–Kutta–Verner fifth-order and sixth-order method (IMSL Library, subroutine DIVPRK), and, in order to satisfy the boundary condition (22.2) at $\vartheta = \pi$, iterations are performed by using the modified Powell hybrid algorithm (IMSL Library, subroutine DNEQNF).

3.4. Elastic unloading and plastic reloading in the crack wake

As in [8], the motion of the material points close to the trajectory of the crack tip can be assumed, in the spirit of the infinitesimal theory approximation, to be rectilinear and parallel to the crack-tip trajectory (Figure 2). A generic material point near the trajectory of the crack tip, which experiences plastic loading, elastic unloading and, finally, plastic reloading, is singled out by the angular coordinate ϑ. The conditions under which elastic unloading and plastic reloading occur for the generic material point are the standard loading/unloading conditions of plasticity (20). Consequently, a material particle leaves the plastic loading sector, of angular location ϑ_1, when λ becomes zero. In the elastic unloading sector, the hidden variables $\boldsymbol{\alpha}$ and k keep the same values they had at unloading. Therefore, (16) reduces to the ODEs governing stationary crack propagation in a linear isotropic elastic material ((16.4–16.6) simply give the conditions $\dot{\boldsymbol{\alpha}} = \dot{\sigma}_e = 0$). Finally, plastic reloading adjacent to the crack flanks occurs at angle ϑ_2, when the yield condition (1) is satisfied.

Table 1. Values of the singularity exponent s, elastic unloading and plastic reloading angles ϑ_1 and ϑ_2, for different values of the hardening ratio: $\alpha = 0.1, 0.01$ and 0.001

α		0.1			0.01			0.001	
b	s	ϑ_1	ϑ_2	s	ϑ_1	ϑ_2	s	ϑ_1	ϑ_2
1.00	−0.20716	69.823		−0.07325	52.874	179.947	−0.02444	42.916	179.837
0.80	−0.18436	80.852	179.999	−0.06334	65.069	179.821	−0.02089	55.681	179.603
0.60	−0.15920	99.596	179.804	−0.05327	84.515	178.785	−0.01740	76.166	178.125
0.55	−0.15462	105.826	179.318	−0.05180	90.669	177.349	−0.01690	82.568	176.274
0.50	−0.15226	112.892	177.420	−0.05197	98.494	171.500	−0.01728	92.524	165.129
0.45	−0.15519	122.482	160.399	−0.06178			−0.04227		
0.40	−0.16550			−0.09035			−0.08143		
0.30	−0.18911			−0.15842			−0.15555		
0.20	−0.22641			−0.21937			−0.21898		
0.10	−0.26182			−0.27070			−0.27190		

3.5. Continuity of the stress function

It may be observed that the stress component T_r could, in principle, suffer jumps. If this were the case, the above described solution procedure should be modified to take these possibilities of jumps into account. However, these jumps have been exculded for elastoplastic materials obeying the Drucker stability postulate, initially for a wide class of hardening rules [20] and recently for any kind of non-softening hardening rules [21]. Therefore, stress jumps are a priori excluded in the present context, and we will find in fact continuous solutions in all our numerical results.

4. Results

The values of the field singularity s, of the elastic unloading angle ϑ_1, and of the plastic reloading angle ϑ_2, are reported in Table 1 (for $\alpha = 0.1, 0.01$, and 0.001), for various values of the mixity parameter b. Note that for sufficiently small b the elastic sector vanishes. The angular distributions of the functions $T_r, T_\vartheta, A_r, A_\vartheta$ and T_c are reported in Figure 3 (for $\alpha = 0.1$) and in Figure 4 (for $\alpha = 0.001$), for different values of the mixity parameter b. Function w, divided by s, is reported in Figure 5, whereas the field singularity s and the unloading and reloading angles are reported in Figure 6 and 7, respectively.

In the case of $b = 1$, the results reduce to those obtained in [8]. From tables and figures it can be appreciated that the most evident effect of hardening anisotropy is the vanishing of the elastic unloading sector in the crack wake. In contrast to the isotropic hardening case, when b is small enough continued yielding occurs when the crack tip leaves the material point behind it. This effect was noted [15], using a finite element simulation of crack growth. Moreover, Lam and McMeeking [22] and Narasimhan et al. [15] found a radial variation of the near crack-tip fields in the form of r^s, which validates the assumption (15).

In Figure 8(a, b) (for $\alpha = 0.1$ and 0.001, respectively) the stress and back stress history is reported for a material particle at a fixed distance, say a, from the crack tip, displaying

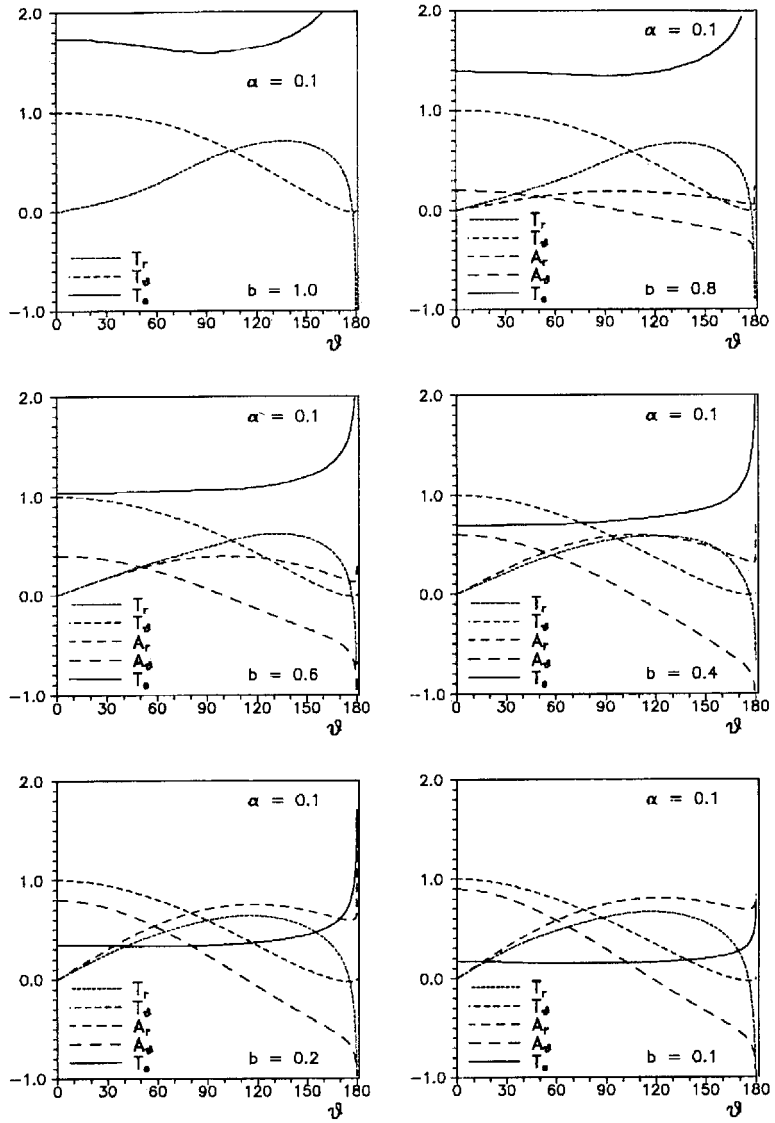

Figure 3. Near crack-tip angular distribution of stress T_r, T_ϑ, back stress A_r, A_ϑ and current flow stress T_e for high hardening ratio $\alpha = 0.1$. Different values of the mixed hardening parameter b are considered.

isotropic ($b = 1$) and mixed ($b = 0.1$) hardening. In particular, the following relations can be obtained from the condition of rectilinear path of the material particle

$$\begin{aligned} \frac{\sigma_{31}}{G}\left(\frac{a}{B}\right)^{-s} &= (T_r \cos\vartheta - T_\vartheta \sin\vartheta)(\sin\vartheta)^{-s}, \\ \frac{\sigma_{32}}{G}\left(\frac{a}{B}\right)^{-s} &= (T_r \sin\vartheta + T_\vartheta \cos\vartheta)(\sin\vartheta)^{-s}, \end{aligned} \tag{29}$$

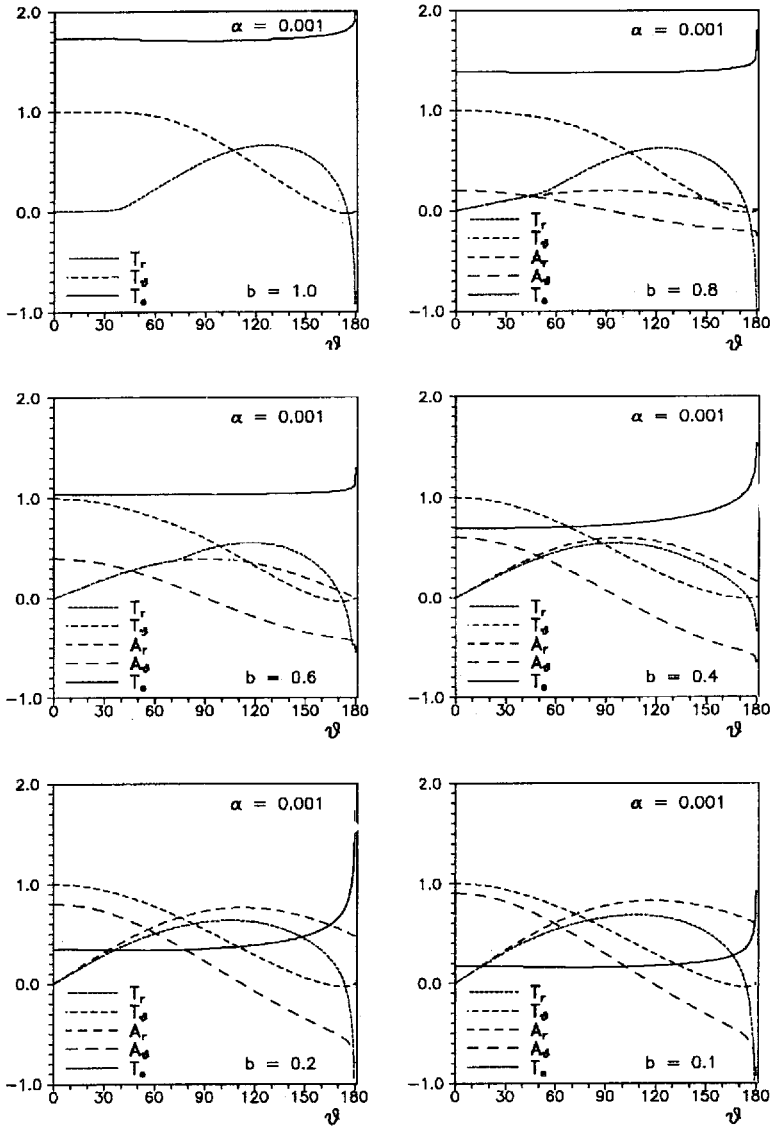

Figure 4. As for Figure 3, except that $\alpha = 0.001$.

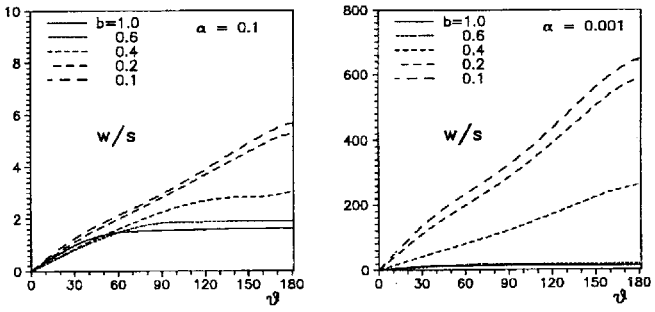

Figure 5. Near crack-tip angular distribution of velocity w (scaled by the singularity exponent s) for different hardening ratios $\alpha = 0.1$ and $\alpha = 0.001$. Different values of the mixed hardening parameter b are considered.

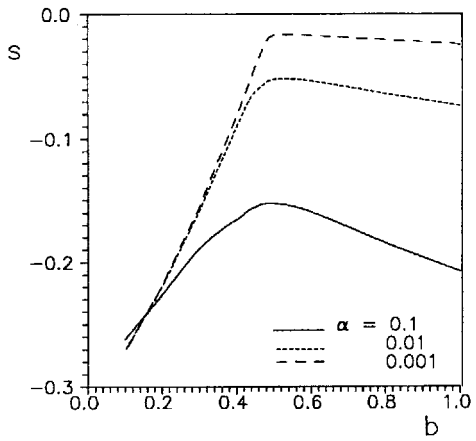

Figure 6. Variation of the stress and velocity singularity s with respect to the mixed hardening parameter b, for different hardening coefficients $\alpha = 0.1$, $\alpha = 0.01$, and $\alpha = 0.001$.

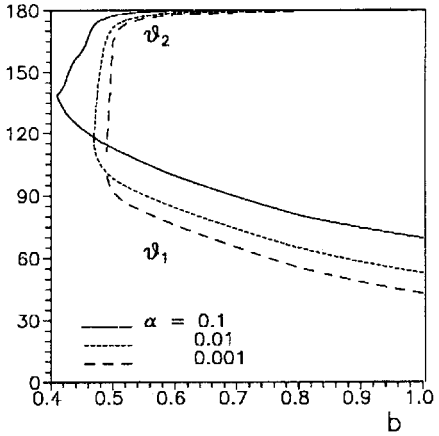

Figure 7. Variation of the elastic unloading (ϑ_1) and plastic reloading (ϑ_2) angles with the mixed hardening parameter b, for different hardening coefficients $\alpha = 0.1$, $\alpha = 0.01$, and $\alpha = 0.001$.

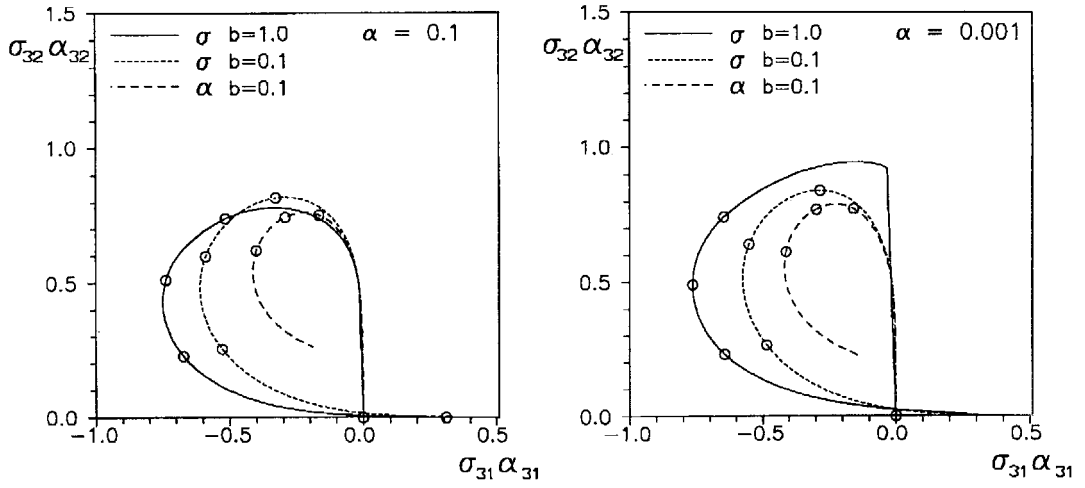

Figure 8. Stress history experienced by a material particle for $\alpha = 0.1$ (small circles denote the particle positions $\vartheta = 0, \pi/4, \pi/2, 3\pi/4, \pi$).

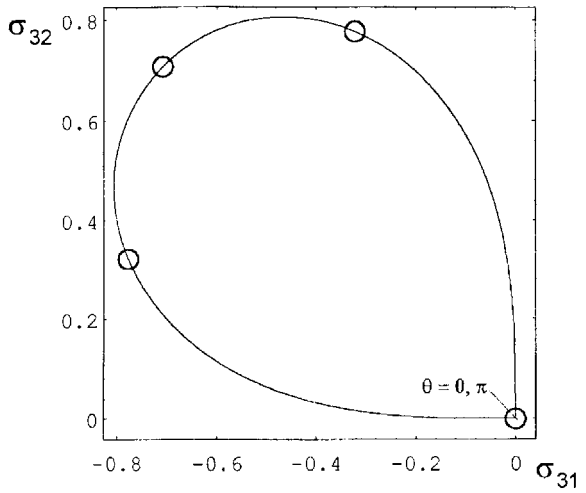

Figure 9. As for Figure 8, in the limiting case of pure kinematic hardening: leading order term.

$$\begin{aligned}\frac{\alpha_{31}}{G}\left(\frac{a}{B}\right)^{-s} &= (A_r \cos\vartheta - A_\vartheta \sin\vartheta)(\sin\vartheta)^{-s},\\ \frac{\alpha_{32}}{G}\left(\frac{a}{B}\right)^{-s} &= (A_r \sin\vartheta + A_\vartheta \cos\vartheta)(\sin\vartheta)^{-s}.\end{aligned} \tag{30}$$

Relations (29) and (30) have been used to obtain the plots of Figure 8 (σ_{3i} and α_{3i} have been reported for simplicity in the figure, instead of terms on the left-hand side of (29) and (30)), where small circles indicate the particle position at fixed angles ($\vartheta = 0, \pi/4, \pi/2, 3\pi/4$ and π). It can be observed that the material particle is in a stress-free state when it lies at an infinite distance ahead of the crack tip ($\vartheta = 0$), it experiences almost proportional loading before $\vartheta = \pi/4$, then it suffers a strongly non proportional stress history and, finally, it approaches a finite value of stress at infinite distance behind the crack tip, for $\vartheta = \pi$ (this tendency to a finite value of stress on the crack flanks is clearly elucidated in [19], and the same arguments apply in the present context). If we consider that our asymptotic solution is known except for an amplitude factor, Figure 9 shows impressive agreement with the numerical finite element results of [15] (their Figure 4).

From the results above, it can be further observed that the angular stress distribution for mixed hardening does not deviate significantly from isotropic hardening under mode III loading conditions. The main differences in the stress distribution occur ahead of the crack tip, in the sector between 0° and 90°, where, for kinematic hardening, a decrease of T_ϑ with ϑ, corresponding to an increase of T_r, is observed. Moreover, when ϑ tends to π, T_r approaches a negative value, as noted in [8] for isotropic hardening and in [15] for kinematic hardening. There are however other effects related to an increase in the kinematic component of hardening. In particular (Figure 6), the strength of the singularity (i.e. the modulus of s) slightly decreases with b, it reaches a minimum for b around 0.5 and then it increases and tends to the value of the elastic singularity (-0.5) in the limit $b \to 0$. Moreover (see Figure 5), the velocity angular function tends to increase with decreasing b at the crack flanks, and this is consistent with the crack opening profiles obtained in [15], which suggest that the CTOD is larger for kinematic than for isotropic hardening.

It can be finally observed from Figures 4, 5 and 7 that *the solution tends to an elastic solution in the limit* $b \to 0$. This tendency is fully confirmed by the analytical solution obtained in the next section.

5. Pure kinematic hardening limit

It should be noted that the formulation presented in Section 3 does not hold in the limiting case of pure kinematic hardening, i.e. for $b = 0$. In this case, the yield surface translates – without any change in dimensions – in the stress space to an infinte distance from the origin. It can therefore be appreciated that, in this limiting case, $T_r(0)$ and $T_\vartheta(0)$ coincide with $A_r(0)$ and $A_\vartheta(0)$, respectively, and the first order approximation (15) is not sufficient to represent the asymptotic solution. A higher order analysis is required, which, as suggested by numerical results of Section 4, yields for the leading order term, the asymptotic solution for a crack steadily running in a linear elastic material having shear modulus G_t. The analysis also provides the second order terms, resulting independent of r. This result, which represents the first higher order analytical solution for a crack steadily moving in an elastoplastic material, is obtained in the following.

Instead of representation (15), we adopt the higher order representation

$$\begin{aligned}
\sigma_{3\alpha}(r,\vartheta) &= G\left[\left(\frac{r}{B}\right)^{s} T_\alpha(\vartheta) + S_\alpha(\vartheta) + \left(\frac{r}{B}\right)^{-s} R_\alpha(\vartheta) + \cdots\right], \\
\alpha_{3\alpha}(r,\vartheta) &= G\left[\left(\frac{r}{B}\right)^{s} T_\alpha(\vartheta) + H_\alpha(\vartheta) + \left(\frac{r}{B}\right)^{-s} P_\alpha(\vartheta) + \cdots\right], \\
v_3(r,\vartheta) &= c\left[\left(\frac{r}{B}\right)^{s} \frac{w(\vartheta)}{s} + u(\vartheta) + \cdots\right],
\end{aligned} \tag{31}$$

where the index α stands for r or ϑ. The two singular terms in the representation of the stress and the back stress are identical, and this is necessary to keep the reduced stress finite, in the limit $r \to 0$. For pure kinematic hardening ($b = 0$), the current yield stress σ_e is a constant. Moreover, the reduced stress becomes

$$\frac{\tilde{\sigma}_{3\alpha}(r,\vartheta)}{G} = \tilde{S}_\alpha(\vartheta) + \left(\frac{r}{B}\right)^{-s} \tilde{R}_\alpha(\vartheta), \tag{32}$$

where

$$\tilde{S}_\alpha = S_\alpha - H_\alpha, \qquad \tilde{R}_\alpha = R_\alpha - P_\alpha. \tag{33}$$

A substitution of (32) into the yield condition (1) gives

$$\tilde{S}_r^2 + \tilde{S}_\vartheta^2 = k^2, \qquad \tilde{S}_r \tilde{R}_r + \tilde{S}_\vartheta \tilde{R}_\vartheta = 0, \tag{34}$$

at second and third order, respectively. Note that terms $O(r^{-2s})$ does not enter the yield condition at third order, because the singular term is null in representation (32). In (34), the non-dimensional parameter $k = \sigma_e/(\sqrt{3}G)$ has been introduced

When the stress fields (31.1) are substituted in the quasistatic equilibrium equation (8), Eqn. (16.1) is recovered for the singular term, and for the second order term we obtain

$$S_{\vartheta,\vartheta} + S_r = 0. \tag{35}$$

The constitutive equations (9) and (10), for pure kinematic hardening ($b = 0$) give

$$2G\dot{\varepsilon}_{3\alpha} = \dot{\sigma}_{3\alpha} + (\alpha^{-1} - 1)\dot{\alpha}_{3\alpha}, \tag{36}$$

$$\dot{\alpha}_{3\alpha} = \frac{1}{k^2 G^2}\langle \tilde{\sigma}_{3r}\dot{\sigma}_{3r} + \tilde{\sigma}_{3\vartheta}\dot{\sigma}_{3\vartheta}\rangle \tilde{\sigma}_{3\alpha}. \tag{37}$$

Let us assume plastic loading everywhere in the crack flanks (we will show later that in fact this condition can always be verified). The deformation, stress, and back stress rates, (12–14) may be written in terms of fields (31), and these expressions can be substituted into the constitutive equation (36) and (37). Therefore, at first order, (36) gives

$$\alpha w = \Sigma_r, \qquad \alpha w_{,\vartheta} = s\Sigma_\vartheta, \tag{38}$$

and at second order

$$\tilde{S}_{r,\vartheta} - \tilde{S}_\vartheta + \alpha^{-1}(H_{r,\vartheta} - H_\vartheta) = 0, \tag{39}$$

$$u_{,\vartheta} = (\alpha^{-1} - 1)(H_{\vartheta,\vartheta} + H_r)\sin\vartheta. \tag{40}$$

Moreover, (37) at first order gives

$$k^2\Sigma_\alpha = (\tilde{S}_r\Sigma_r + \tilde{S}_\vartheta\Sigma_\vartheta)\tilde{S}_\alpha, \tag{41}$$

and at seconds order

$$\begin{aligned}(H_{r,\vartheta} - H_\vartheta)k^2 \sin\vartheta &= (S_{r,\vartheta} - S_\vartheta)\tilde{S}_r^2 \sin\vartheta + (\tilde{S}_r\Sigma_r + \tilde{S}_\vartheta\Sigma_\vartheta)\tilde{R}_r,\\ (H_{\vartheta,\vartheta} + H_r)k^2 \sin\vartheta &= (S_{r,\vartheta} - S_\vartheta)\tilde{S}_r\tilde{S}_\vartheta \sin\vartheta + (\tilde{S}_r\Sigma_r + \tilde{S}_\vartheta\Sigma_\vartheta)\tilde{R}_\vartheta.\end{aligned} \tag{42}$$

It must be noted that (42) determines the higher order terms $\tilde{R}_r$ and $\tilde{R}_\vartheta$, when S_r, S_ϑ, H_r and H_ϑ are known.

From equilibrium and constitutive equations (16.1) and (38), it can be concluded that the angular stress and velocity functions for the singular terms coincide with the crack-tip fields in an elastic solid having shear modulus G_t and *stress intensity factor* K_{III}. Taking into account the mode III boundary conditions (21) we have

$$\begin{aligned}&s = -\tfrac{1}{2}, \qquad \sqrt{B} = \frac{K_{\mathrm{III}}}{G\sqrt{2\pi}},\\ &T_\vartheta = \cos\frac{\vartheta}{2}, \qquad T_r = \sin\frac{\vartheta}{2}, \qquad w = -\frac{1}{2\alpha}\sin\frac{\vartheta}{2},\end{aligned} \tag{43}$$

$$\Sigma_r = -\tfrac{1}{2}\sin\frac{\vartheta}{2}, \qquad \Sigma_\vartheta = \tfrac{1}{2}\cos\frac{\vartheta}{2}. \tag{44}$$

Equations (44), (41) and (34) determine $\tilde{S}_r$ and $\tilde{S}_\vartheta$, except for the sign, which is determined by the plastic loading condition dev $\tilde{\boldsymbol{\sigma}}\cdot\dot{\boldsymbol{\sigma}} > 0$. Therefore

$$\tilde{S}_r = -k \sin\frac{\vartheta}{2}, \qquad \tilde{S}_\vartheta = k \cos\frac{\vartheta}{2}. \tag{45}$$

Note that the plastic loading condition is verified at every value of ϑ. Therefore, the zone around the crack tip is fully plastic, without any elastic unloading sector.

By using the definition (31.1), a substitution of (45) for the stress components S_r and S_ϑ, into the equilibrium equation (37) gives the differential equation

$$H_{\vartheta,\vartheta} + H_r = \tfrac{3}{2}k \sin\frac{\vartheta}{2}. \tag{46}$$

Moreover, a substitution of the results in (45) into (39), gives

$$H_{r,\vartheta} - H_\vartheta = \tfrac{3}{2}\alpha k \cos\frac{\vartheta}{2}. \tag{47}$$

The system of ODEs (46–47) can be integrated to obtain

$$\begin{aligned} H_r &= A_1 \sin\vartheta + A_2 \cos\vartheta + (2-\alpha)k \sin\frac{\vartheta}{2}, \\ H_\vartheta &= A_1 \cos\vartheta - A_2 \sin\vartheta + (1-2\alpha)k \cos\frac{\vartheta}{2}, \end{aligned} \tag{48}$$

where A_1 and A_2 are arbitrary constants. Finally, the boundary conditions (21) imply $A_1 = A_2 = 0$. Moreover, the second order stress function S_r and S_ϑ can be obtained by substituting (48) into (45), and the velocity function u can be obtained by integrating (40). Therefore the stress, back stress and velocity fields (31) near to the crack tip become

$$\sigma_{3r} = \left[\frac{K_{\mathrm{III}}}{\sqrt{2\pi r}} + k(G - G_t)\right] \sin\frac{\vartheta}{2}, \qquad \sigma_{3\vartheta} = \left[\frac{K_{\mathrm{III}}}{\sqrt{2\pi r}} + 2k(G - G_t)\right] \cos\frac{\vartheta}{2}, \tag{49}$$

$$\alpha_{3r} = \left[\frac{K_{\mathrm{III}}}{\sqrt{2\pi r}} + k(2G - G_t)\right] \sin\frac{\vartheta}{2}, \qquad \alpha_{3\vartheta} = \left[\frac{K_{\mathrm{III}}}{\sqrt{2\pi r}} + k(G - 2G_t)\right] \cos\frac{\vartheta}{2}, \tag{50}$$

$$v_3 = \frac{c}{G_t}\left[\frac{K_{\mathrm{III}}}{\sqrt{2\pi r}} + 2k(G - G_t)\left(\sin\frac{\vartheta}{2}\right)^2\right] \sin\frac{\vartheta}{2}, \tag{51}$$

where (43.2) has been used.

The form of leading order terms of fields (49–51) is identical to the leading order terms of the linear isotropic elastic case. It is worth noting that the second order terms of fields (49–51) are different from the linear elastic case, where terms independent of r are not present. In particular, the stress and back stress components have the same dependence on ϑ at first and second order. The stress history of the generic particle is reported in Figure 9 for the leading order term of the analytical solution (49), employing (29), with $s = -\frac{1}{2}$ (σ_{3i} has been reported in the figure, instead of terms on the left-hand side of (29)). The second order reduced stress history of the generic particle is reported in Figure 10. In Figures 9 and 10, small circles indicate the particle position at fixed angles ($\vartheta = 0, \pi/4, \pi/2, 3\pi/4$ and π; note that the two

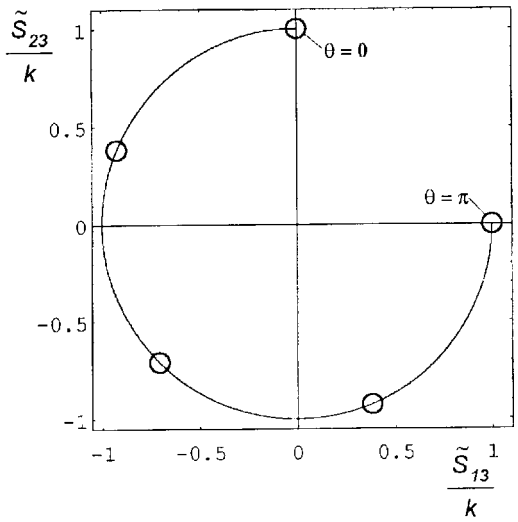

Figure 10. Reduced stress history experienced by a material particle in the limiting case of pure kinematic hardening (small circles denote the particle positions $\vartheta = 0, \pi/4, \pi/2, 3\pi/4, \pi$).

points $\vartheta = 0$ and $\vartheta = \pi$ coincide in Figure 9). Figure 9 is in very good agreement with Figures 8 (a) and (b). As a consequence of the fact that the section of the von Mises yield surface with the π-plane is a circumference, Figure 10 results as an arc of a circumference.

6. Conclusions

The asymptotic solution has been obtained for a crack steadily propagating, under antiplanar shearing conditions in a material characterized by the J_2-flow theory of plasticity with mixed isotropic-kinematic hardening. The solution completes the results on crack propagation in J_2 materials, where mode I, II and III crack propagation solutions were known for isotropic hardening [8–12], whereas only the mode I crack propagation solution was known for anisotropic hardening [14]. Moreover, the limiting case of pure kinematic hardening has been solved, which requires a higher order approximation of crack fields.

The results, which are in very good agreement with the finite element solution [15], show that the anisotropic component of hardening influences in a non-negligible way the asymptotic fields. In particular, it turns out that the elastic unloading sector in the crack wake tends to disappear, and the strength of the singularity and the velocity in the crack wake increase, when the anisotropic component of hardening is increased, namely, for b lower than 0.5. These effects support the conclusion, which was motivated by finite element simulations [15], and is now confirmed by asymptotic analysis, that isotropic hardening based models tend to overestimate the capacity of material to sustain stable crack growth.

Acknowledgments

The authors are grateful to Prof. W.J. Drugan (University of Wisconsin–Madison, U.S.A.) for his valuable comments and helpful discussions. The financial support of the Italian C.N.R. (contr. No 95.00206.07) is gratefully acknowledged.

References

1. J.W. Hutchinson, *Journal of the Mechanics and Physics of Solids* 16 (1968) 13–81.
2. Ibid, 337–347.
3. J.R. Rice and G.F. Rosengren, *Journal of the Mechanics and Physics of Solids* 16 (1968) 1–12.
4. A.D. Chitaley and F.A. McClintock, *Journal of the Mechanics and Physics of Solids* 19 (1971) 147–163.
5. L.I. Slepyan, *Meckanika Tverdogo Tela* 9 (1974) 57–67.
6. W.J. Drugan, J.R. Rice and T.L. Sham, *Journal of the Mechanics and Physics of Solids* 30 (1982) 447–473.
7. J.R. Rice, in *Mechanics of Solids: The Rodney Hill 60th Anniversary Volume*, H.G. Hopkins and M.J. Sewell (eds.) Pergamon Press, Oxford (1982) 539–562.
8. P. Ponte Castãneda, *Journal of the Mechanics and Physics of Solids* 35 (1987) 227–268.
9. J. Amazigo and J.W. Hutchinson, *Journal of the Mechanics and Physics of Solids* 25 (1977) 81–97.
10. D. Bigoni and E. Radi, *International Journal of Solids and Structures* 30 (1993) 899–919.
11. E. Radi and D. Bigoni, *Mechanics of Materials* 14 (1993) 239–251.
12. E. Radi and D. Bigoni, *International Journal of Plasticity* 10 (1994) 761–793.
13. E. Radi and D. Bigoni, *Journal of the Mechanics and Physics of Solids* (1996) in press.
14. R. Zhang, X. Zhang and K.C. Hwang, in *Proceedings of ICF International Symposium on Fracture Mechanics*, Science Press, Beijing (1983) 283–290.
15. R. Narasimhan, C.S. Venkatesha and S. Sairam, *International Journal of Solids and Structures* 30 (1993) 659–673.
16. W. Prager, *Journal of Applied Mechanics, ASME* 23 (1956) 493–496.
17. H. Ziegler, *Quarterly of Applied Mathematics* 17 (1959) 55–65.
18. W. Prager, *Journal of Applied Mechanics, ASME* 20 (1949) 235–241.
19. K. Bose and P. Ponte Castãneda, *Journal of the Mechanics and Physics of Solids* 40 (1992) 1053–1103.
20. W.J. Drugan and J.R. Rice, in *Mechanics of Material Behavior*, G.J. Dvorak and R.T. Shield (eds.) Elsevier, Amsterdam (1984) 59–73.
21. W.J. Drugan, Private communication, 1995.
22. P.S. Lam and R.M. McMeeking, *Journal of the Mechanics and Physics of Solids* 32 (1984) 395–414.